

Quantum mechanical compact modeling of symmetric double-gate MOSFETs using variational approach

P. Vimala[†] and N. B. Balamurugan

Department of Electronics and Communication Engineering, Thiagarajar College of Engineering, Madurai-625015, Tamilnadu, India

Abstract: A physics-based analytical model for symmetrically biased double-gate (DG) MOSFETs considering quantum mechanical effects is proposed. Schrödinger's and Poisson's equations are solved simultaneously using a variational approach. Solving the Poisson and Schrödinger equations simultaneously reveals quantum mechanical effects (QME) that influence the performance of DG MOSFETs. The inversion charge and electrical potential distributions perpendicular to the channel are expressed in closed forms. We systematically evaluated and analyzed the potentials and inversion charges, taking QME into consideration, in Si based double gate devices. The effect of silicon thickness variation in inversion-layer charge and potentials are quantitatively defined. The analytical solutions provide good physical insight into the quantization caused by quantum confinement under various gate biases.

Key words: quantum mechanical effects; DG MOSFETs; centroid; electric potential; inversion-layer charge

DOI: 10.1088/1674-4926/33/3/034001

EEACC: 2570

1. Introduction

Silicon-on-insulator (SOI) has been long known for its superior performance capabilities, and there is an interest in double-gate (DG) and fully depleted silicon-on-insulator (FD/SOI) MOSFETs because of their scalability and superior speed^[1]. Sub 100 nm MOSFET technology will be widely used in device modeling for at least the next 10 years^[2]. Short-channel effects are suppressed via the sub micrometer MOSFETs rather than by extreme channel doping densities and profiles.

The deep sub micrometer MOSFETs of the present generation use very high channel doping and very thin gate oxides to avoid short-channel effects, resulting in very high electric fields at the Si/SiO₂ interface. At such high electric fields a significant bending of the energy-bands at the Si/SiO₂ interface is produced and the potential well becomes narrow enough to quantize the motion of inversion layer carriers in the direction perpendicular to the interface. Due to this quantization, the energy levels are split into subbands, and the lowest of the allowed energy levels for electrons in the well does not coincide with the bottom of the conduction band. For MOSFETs in the threshold region, the reduced gate capacitance resulting from QMEs increases the short-channel effects and lowers the transconductance and drive currents. Thus, for these devices classical theory is no longer sufficient, and QMEs^[3–5] become very important for the accurate modeling of device characteristics.

One important consequence of the quantum mechanical (QM) carrier distribution, with regard to the device behavior, occurs when the silicon thickness is varied, so a reliable compact model for DG-MOSFETs must take into account quantum effects. To suppress the short-channel effects, a thin silicon film t_{si} with thickness < 20 nm is often used, and the

quantum confinement effects can no longer be ignored. It has been shown that QMEs play a crucial role for device operation when the channel thickness is smaller than 20 nm^[6, 7]. Much work has been devoted to modeling the electrostatic features of DG-MOSFETs, which can be categorized as: (i) models relying on a purely classical description^[8–11], which do not include QMEs; (ii) 1D and 2D self-consistent models which numerically solve the coupled Schrödinger and Poisson equations^[12–14], which are ideal for quantitative understanding of the underlying physics but which are not suitable for compact modeling; (iii) models using a perturbation theory—even in the strong inversion region—in which the structural confinement is taken into account, but which are not suitable for dealing with the strong field dependence^[15, 16]; and (iv) models based on a QM variational approach^[17], in which the potential depends on the inversion charge density. These models do not calculate the inversion layer charge based on QM effects, instead, they employ quantum correction using model parameters. Thus, there is scope for developing a simple yet accurate analytical model for inversion layer charge for present day MOS devices considering QMEs.

In this paper, we develop a physical model for QMEs in the threshold region of symmetrical DG-MOSFETs. The details about the double gate and the band diagram are given, and the generation of the quantum analytical model for DG-MOSFET is presented. Also, the inversion charge and inversion layer centroid is modelled in terms of gate voltages.

2. Device physics

In recent years, several technologies have been proposed to keep up with the scaling imposed by Moore's law. Among these innovations are the introduction of new materials in the CMOS process, such as high- k dielectrics, metal gate elec-

[†] Corresponding author. Email: vimalapalanichamy@tce.edu

Received 4 August 2011, revised manuscript received 19 October 2011

© 2012 Chinese Institute of Electronics

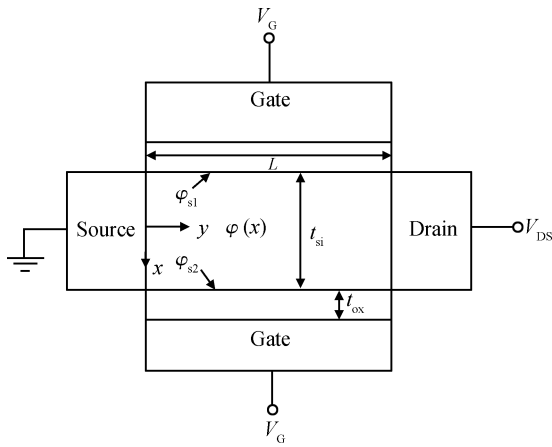


Fig. 1. Cross section of symmetrical DG-MOSFET structure and its coordinate system.

trodes and stressors, which allow the build-up of mechanical stress in the silicon to increase carrier mobility. In addition to these material innovations, new transistor architectures have emerged. A silicon-on-insulator (SOI) transistor is one such example.

SOI has been long known for its superior performance capabilities. Recently, one has witnessed an evolution of the SOI transistor from a classical, planar, single-gate architecture to a three dimensional structure with multiple gates (double-, triple- or quadruple-gate devices). The double-gate MOSFET is considered to be one of the most promising device structures to extend CMOS scaling into the nanometer regime. Figure 1 shows the cross section and coordinate systems of a long symmetrical undoped double gate (DG) nMOSFET. L is the gate length, t_{si} is the silicon film thickness and t_{ox} is the gate-oxide thickness. The key factors that limit how far a DG MOSFET can be scaled come from short-channel effects such as threshold voltage roll-off and drain-induced barrier lowering (DIBL). For $t_{si} \rightarrow 0$, the confinement is in the potential well defined by the front- and back-gate oxide barriers (which are virtually equal to infinity) as illustrated in Fig. 2. Here almost all electrons occupy the ground-state sub-band of the lower ladders, and more than 90% of the total electrons occupy the ground-state sub-band for $t_{si} < 3$ nm. Higher order sub-bands are not important.

3. QM modeling process

For DG and FD/SOI MOSFETs, when the gate is biased at the flat-band voltage, the confinement is in the potential well defined by the front- and back-gate oxide barriers, for which higher-order subbands are important. In this case, the Schrödinger equation can be solved analytically to yield^[18],

$$\psi_j(x) = \sqrt{\frac{2}{t_{si}}} \sin \frac{(j+1)\pi x}{t_{si}}, \quad j = 0, 1, 2, \dots \quad (1)$$

Considering the above equation, the trial eigenfunction for FD/SOI MOSFETs,

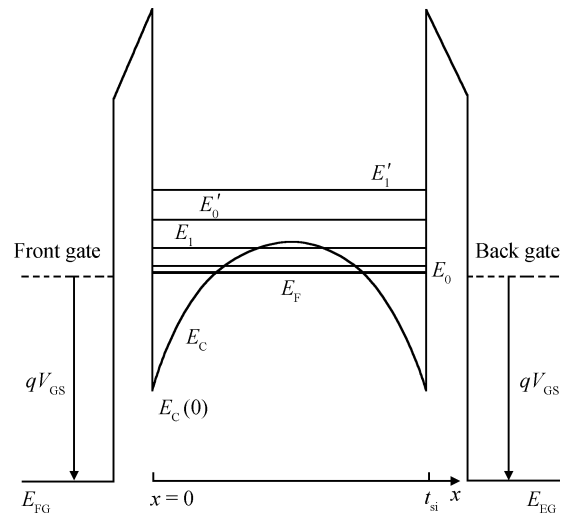


Fig. 2. Schematic energy-band diagram across the thin Si film (channel) of a symmetrical DG nMOSFET with $V_{GS} > 0$ applied to both gates; the quantized electron sub-band energies in the inversion layer are also shown.

$$\psi_j(x) = a_j \sqrt{\frac{2}{t_{si}}} \sin \frac{(j+1)\pi x}{t_{si}} e^{-b_j x/t_{si}}, \quad j = 0, 1, 2, \dots, \quad (2)$$

where b_j is the undetermined parameter and a_j is the normalization constants.

For symmetrical DG MOSFETs, we can extend Eq. (2) and write the trial eigenfunctions as,

$$\psi_j(x) = a_j \sqrt{\frac{2}{t_{si}}} \sin \frac{(j+1)\pi x}{t_{si}} \left(e^{-b_j x/t_{si}} + e^{-b_j (t_{si}-x)/t_{si}} \right), \quad j = 0, 1, 2, \dots \quad (3)$$

Normalization of Eq. (3), $\int_0^{t_{si}} \psi_j^2 dx = 1$; gives

$$a_j = \frac{2}{\sqrt{2e^{-b_j} + \frac{[(j+1)\pi]^2 (1 - e^{-2b_j})}{b_j \{b_j^2 + [(j+1)\pi]^2\}}}}, \quad j = 0, 1, 2, \dots \quad (4)$$

Now we follow the variational approach to simultaneously solve, the Schrödinger equation and Poisson's equation,

$$\begin{aligned} \frac{d^2}{dx^2} \varphi(x) &= \frac{q}{\epsilon_{si}} [N_A + n(x)] \\ &= \frac{q}{\epsilon_{si}} \left[N_A + \sum_j N_j |\psi_j(x)|^2 \right] \\ &= \frac{q}{\epsilon_{si}} \left[N_A + N_{inv} |\psi_j(x)|^2 \right]. \end{aligned} \quad (5)$$

In Eq. (5), $\varphi(x)$ is the electric potential in the silicon film, N_j is the inversion-electron areal density in the j th sub-band, N_{inv} is the total inversion-electron density, and $\psi_j(x)$ is the

eigenfunction. In order to solve Eq. (5), we need an approximation for $\psi_j(x)$. Use $\psi_j(x)$ as $\psi_0(x)$, the lowest-energy sub-band eigenfunction ($j = 0$). The electrostatic potential in the Si film is obtained by integrating Eq. (5) twice from $x = 0$ to t_{si} :

$$\begin{aligned} \varphi(x) = & \frac{Q_d}{2\varepsilon_{\text{si}}} \left(\frac{x^2}{t_{\text{si}}} - x \right) + \frac{t_{\text{si}} Q_{\text{inv}} a_0^2}{4\varepsilon_{\text{si}}} \\ & \times \left[\frac{1}{4b_0^2} \left(e^{-\frac{2b_0 x}{t_{\text{si}}}} + e^{-\frac{2b_0(t_{\text{si}}-x)}{t_{\text{si}}}} \right) \right. \\ & + e^{-b_0} \left(\frac{x^2}{t_{\text{si}}^2} - \frac{x}{t_{\text{si}}} - \frac{1}{\pi^2} \sin^2 \frac{\pi x}{t_{\text{si}}} \right) \\ & + \frac{e^{-\frac{2b_0 x}{t_{\text{si}}}}}{4(\pi^2 + b_0^2)^2} \left((\pi^2 - b_0^2) \cos \frac{2\pi x}{t_{\text{si}}} + 2\pi b_0 \sin \frac{2\pi x}{t_{\text{si}}} \right) \\ & + \frac{e^{-\frac{2b_0(t_{\text{si}}-x)}{t_{\text{si}}}}}{4(\pi^2 + b_0^2)^2} \left((\pi^2 - b_0^2) \cos \frac{2\pi x}{t_{\text{si}}} - 2\pi b_0 \sin \frac{2\pi x}{t_{\text{si}}} \right) \\ & \left. - \frac{\pi^2(\pi^2 + 3b_0^2)(1 + e^{-2b_0})}{4\pi^2(\pi^2 + b_0^2)^2} \right], \end{aligned} \quad (6)$$

where $Q_d = q t_{\text{si}} N_A$ is the depletion charge density and $Q_{\text{inv}} = q N_{\text{inv}}$ is the inversion charge density. The boundary conditions for integration are,

$$\varepsilon_{\text{ox}} \frac{V_{\text{g1}} - V_{\text{fb}} - \varphi_{\text{s1}}}{t_{\text{ox1}}} = -\varepsilon_{\text{si}} \frac{d\varphi}{dx} \Big|_{x=0}, \quad (7)$$

$$\varepsilon_{\text{ox}} \frac{V_{\text{g2}} - V_{\text{fb}} - \varphi_{\text{s2}}}{t_{\text{ox2}}} = -\varepsilon_{\text{si}} \frac{d\varphi}{dx} \Big|_{x=t_{\text{si}}}, \quad (8)$$

where

$$\varphi(x) = \varphi_{\text{s1}} = 0 \quad \text{at} \quad x = 0,$$

$$\varphi(x) = \varphi_{\text{s2}} = 0 \quad \text{at} \quad x = t_{\text{si}}.$$

The one dimensional (1-D) Schrodinger equation is written as,

$$-\frac{\hbar^2}{8\pi^2 m_x} \frac{d^2}{dx^2} \psi_j(x) + (-q)\varphi(x)\psi_j(x) = E_j \psi_j(x), \quad (9)$$

where $\hbar = 6.63 \times 10^{-34}$ J-s is the Plank's constant, E_j are the sub-band energies, and m_x is the effective mass of electrons in the x -direction.

In the effective mass approximation the valleys are generated in pairs. The six valleys split into two groups of sub-bands (known as two ladders). The lower set of sub-bands (unprimed ladder) is 2-fold degenerate and represents those ellipsoids that respond with a heavy longitudinal effective mass ($m_L = 0.916m_0$) in the gate confinement direction while the higher set of sub-bands (primed ladder) is 4-fold degenerate and represents those ellipsoids that respond with a light transverse effective mass ($m_H = 0.19m_0$). Because of the heavier longitudinal mass, the unprimed sub-bands have relatively lower bound-state energies as compared to the primed sub-bands, and are therefore primarily occupied by electrons. Based on the quantum mechanical variational approach, b_j is evaluated by $dE_j/db_j = 0$. With approximation b_j is derived as,

$$b_j = t_{\text{si}} \left[\frac{q m_x \pi^2 (Q_d + \frac{5}{6} Q_{\text{inv}})}{(j+1)\varepsilon_{\text{si}} \hbar^2} \right]^{1/3}. \quad (10)$$

4. Model for inversion charge and centroid

In FD-SOI MOSFETs, the center of the Si film is the maximum carrier-concentration point. With increasing V_{gs} , this point converts to the minimum carrier-concentration point as the two channels are formed. An onset condition for volume inversion can thus be defined by $d^2\psi^2/dx^2 = 0$ at $x = t_{\text{si}}/2$ with $\psi \cong \psi_0$ gives $b_0 \cong \pi$ from Eq. (9). The inversion charge should then be obtained and the device under bias condition. For optimal DG MOSFET design, we need to ensure that the inversion condition defined above is met at the device where $V_{\text{gs}} \cong V_{\text{dd}}$. Therefore, Q_{inv} must relate to V_{gs} .

The inversion-charge density can be related to the gate voltage as follows^[19]:

$$Q_{\text{inv}} = 2C_{\text{ox}}^1 (V_{\text{gs}} - V_t), \quad (11)$$

where

$$C_{\text{ox}}^1 = \frac{C_{\text{ox}}}{1 + C_{\text{ox}} \frac{x_1}{\varepsilon_{\text{si}}}}, \quad (12)$$

$$V_t = \varphi_{\text{ms}} + \varphi_{\text{dep}} + \frac{Q_d}{C_{\text{ox}}}. \quad (13)$$

With $\varphi_{\text{dep}} = \varphi_s - \frac{x_1 Q_{\text{inv}}}{\varepsilon_{\text{si}}}$ is the depletion potential, $C_{\text{ox}} = \varepsilon_{\text{ox}}/t_{\text{ox}}$ is the gate oxide capacitance, x_1 is the inversion layer centroid, φ_{ms} is the work function difference between gate and silicon film, and V_t is a constant threshold voltage for strong inversion.

The inversion layer centroid is given by,

$$x_1 = 2 \int_0^{t_{\text{si}}/2} \psi^2(x) dx. \quad (14)$$

At, $\psi \cong \psi_0$ gives $b_0 \cong \pi$. The onset of strong volume inversion is defined with $b_0 \cong \pi$ and hence $x_1 \cong t_{\text{si}}/\pi$.

5. Results and discussion

To verify the compact quantum model and to give an insight into the quantum effects in DG MOSFETs, we applied it to a variety of Si film thickness of symmetrical DG MOSFETs. The results are compared with SCHRED^[20], which numerically and self-consistently solves the Poisson and Schrödinger equations. Consider n-channel devices with metal (Al with $\varphi_m = 4.10$ eV) gates, oxide thickness $t_{\text{oxf}} = t_{\text{oxb}} = 1.5$ nm, $N_A = 10^{17}$ cm⁻³ and $t_{\text{si}} = 1-20$ nm. Figure 3 shows the model predicted eigenvalues versus the normalized position across the Si film, compared with SCHRED predictions. Also we show the lowest-energy sub-band eigenfunction ψ_0 for $t_{\text{si}} = 5$ nm under different bias conditions. In all bias conditions, the model predictions agree well (almost exactly) with those of SCHRED. Figure 4 shows model and SCHRED predicted electric potentials versus the normalized position for $t_{\text{si}} = 5$ nm

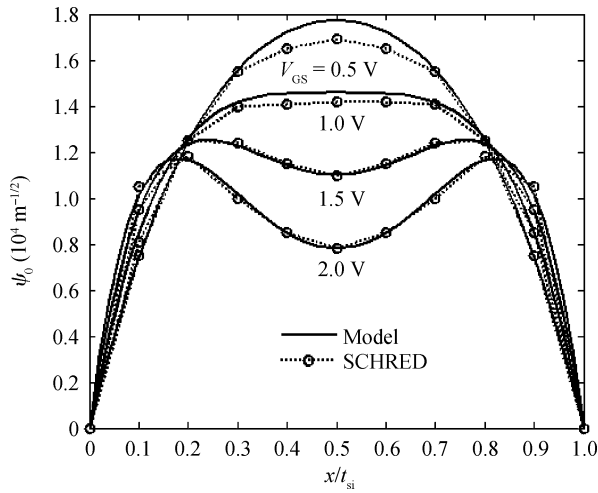


Fig. 3. Model and SCHRED-predicted eigenfunctions normalized position in the Si film. Lowest energy sub-band eigenfunctions for $t_{\text{Si}} = 5 \text{ nm}$ under different values of V_{GS} (different bias conditions).

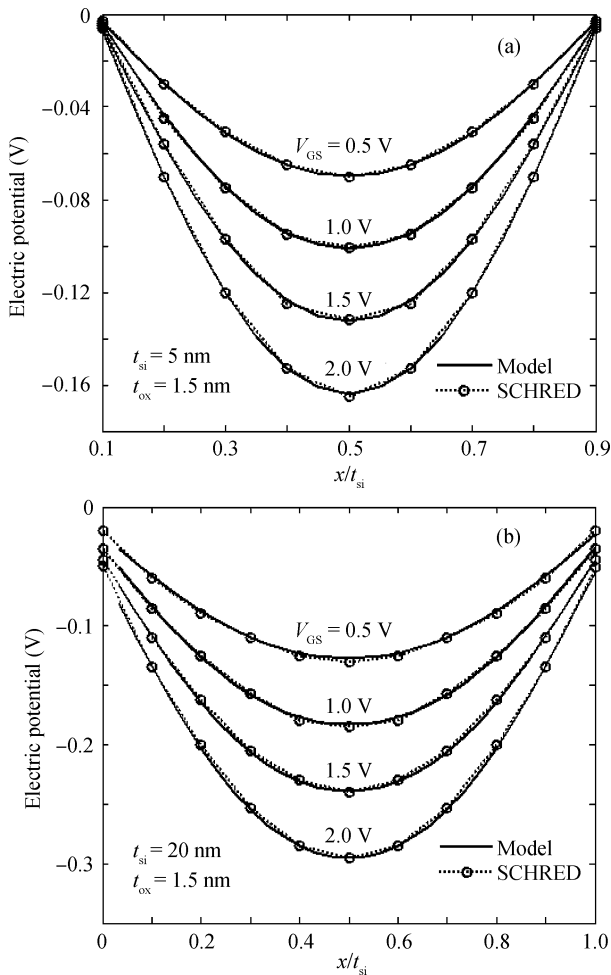


Fig. 4. Electrical potential versus normalized position in the silicon film of symmetrical DG nMOSFETs for (a) $t_{\text{Si}} = 5 \text{ nm}$, (b) $t_{\text{Si}} = 20 \text{ nm}$ under different bias conditions.

and $t_{\text{Si}} = 20 \text{ nm}$ under different bias conditions. The magnitude of the electric potential can be elevated by applying various gate-source voltages. The model predictions are very good

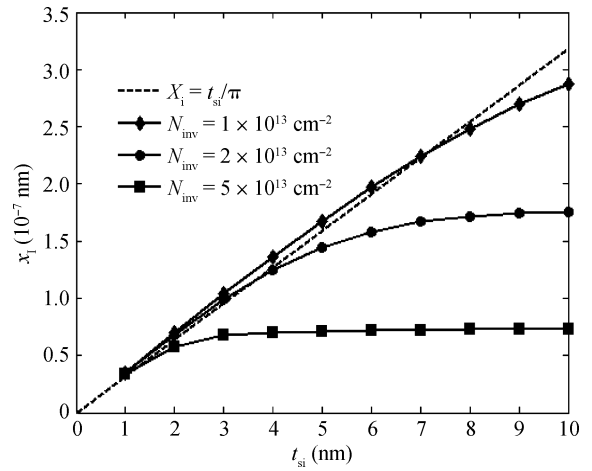


Fig. 5. Average inversion layer centroid versus Si-film thickness for different total inversion-electron densities in symmetrical DG nMOS-FETs.

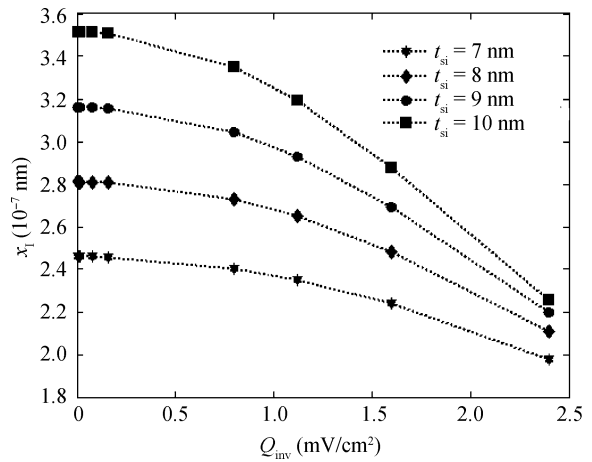


Fig. 6. Average inversion layer centroid versus inversion charge for various values of silicon thicknesses.

approximations for all regions of device operation (for weak (low V_{GS}) as well as strong (high V_{GS}) inversion). The predicted potentials agree very well with SCHRED for $t_{\text{Si}} = 5 \text{ nm}$ and under different values of V_{GS} .

It is to be noted that at the strong inversion, as defined with reference to the previous section, $b_0 \cong \pi$ and hence $x_1 \cong t_{\text{Si}}/\pi$. Figure 5 shows, x_1 in Eq. (15) versus t_{Si} for different N_{inv} and the line corresponding to $x_1 = t_{\text{Si}}/\pi$. For relatively thicker t_{Si} , the symmetrical DG MOSFET operates with two distinct channels, and x_1 decreases with increasing N_{inv} due to the electric field-governed confinement as in the bulk-Si MOSFET^[1]. For a given N_{inv} , x_1 is virtually independent of t_{Si} . For relatively thin t_{Si} , the DG device operates with inversion, and $x_1 \cong t_{\text{Si}}/\pi$ independent of N_{inv} . Thus, for given N_{inv} with inversion (thin t_{Si}), x_1 increases linearly with t_{Si} .

Figure 6 shows the inversion charge centroid versus inversion charge for different values of t_{Si} . It can be seen that the centroid value decreases as the inversion charge increases since the charge distribution shifts toward the Si/SiO₂ interface. Figure 7 illustrates the effect of quantum confinement in DG MOSFETs by plotting the inversion layer charge versus the

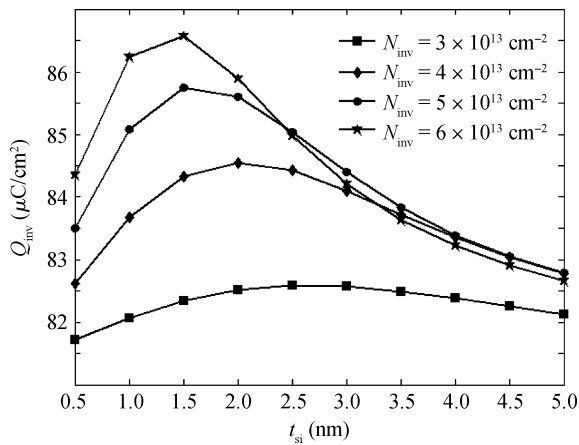


Fig. 7. Channel charge of DG MOSFET as a function of silicon thickness for several values of N_{inv} .

silicon film thickness with various inversion electron concentrations. The results shown in the figure represent the inversion layer charge data obtained analytically by means of Eq. (13). Similar to bulk MOSFETs, quantization in DG MOSFETs also leads to discrete electron sub-bands higher than the bottom of the conduction band and the electron concentration peaks away from the surface. Also it shows that inversion charge increases linearly with increasing N_{inv} . For thin t_{si} , the inversion charge increases linearly up to a particular limit, and decreases linearly for high t_{si} values.

6. Conclusion

A compact physics-based quantum-effects model for symmetric DG MOSFETs of arbitrary Si-film thickness has been developed and demonstrated. The QME is more pronounced in the ultrathin silicon film. Due to the quantum effect, the channel charge carrier density is lower than the classical one. We have developed a model to calculate the inversion charge of DG MOSFETs, where quantum effects are included. The model, based on the quantum mechanical variational approach, accounts for the Si-film thickness dependence with electric potential, inversion charge, centroid and inversion charge. A design criterion for achieving a beneficial strong volume-inversion operation in DG devices was quantitatively defined. The model predictions are a very good approximation for all regions of device operation (for weak (low V_{gs}) as well as strong (high V_{gs}) inversion). Therefore, the model of this work provides a useful method to study QME on DG MOSFETs. DG MOSFETs can be symmetrical or asymmetrical. For asymmetrical DG MOSFETs, the front and back gate materials and/or the gate oxide thicknesses are different. Our QM model may be extended to the asymmetrical DG MOSFETs.

References

- [1] Fossum J G, Ge L, Chiang M H. Speed superiority of scaled double-gate CMOS. *IEEE Trans Electron Devices*, 2002, 49(5): 808
- [2] Semiconductor Industry Association. International Technology Roadmap for Semiconductors, 2010
- [3] Stern F, Howard W E. Properties of semiconductor surface inversion layer in the electric quantum limit. *Phys Rev*, 1967, 163(3): 816
- [4] Stern F. Self-consistent results for n-type Si inversion layers. *Phys Rev B*, 1972, 5(12): 4891
- [5] Pals J A. Experimental verification of the surface quantization of an n-type inversion layer of silicon at 300 and 77 K. *Phys Rev B*, 1972, 5(10): 4208
- [6] Baccarani G, Reggiani S. A compact double-gate MOSFET model comprising quantum-mechanical and nonstatic effects. *IEEE Trans Electron Devices*, 1999, 46(8): 1656
- [7] Taur Y, Buchanan D A, Chen W, et al. CMOS scaling into the nanometer regime. *Proc IEEE*, 1997, 85(4): 486
- [8] Moldovan O, Jiménez D, Guitart J R, et al. Explicit analytical charge and capacitance models of undoped doublegate MOSFETs. *IEEE Trans Electron Devices*, 2007, 54(7): 1718
- [9] Moldovan O, Cerdeira A, Jiménez D, et al. Compact model for highly-doped double-gate SOI MOSFETs targeting baseband analog applications. *Solid-State Electron*, 2007, 51: 655
- [10] Moldovan O, Chaves F A, Jiménez D, et al. Compact charge and capacitance modeling of undoped ultra-thin-body (UTB) SOI MOSFETs. *Solid-State Electron*, 2008, 52: 1867
- [11] Taur Y. Analytic solutions of charge and capacitance in symmetric and asymmetric double-gate MOSFETs. *IEEE Trans Electron Devices*, 2001, 48: 2861
- [12] Majkusiak B, Walczak J. Simulation of the gate tunnel current in the double gate (DG) MOS transistor. *J Comput Electron*, 2006: 143
- [13] Fiegna C, Abramo A. Solution of 1-D Schrodinger and Poisson equations in single and double gate SOI MOS. *Proc SISPAD*, 1997: 93
- [14] Alam M K, Khosrum Q D M. Self-consistent modeling of ultra thin body double gate MOSFET. *IEEE Conference on Electron Devices and Solid State Circuits*, 2007: 601
- [15] Baccarani G, Reggiani S. A compact double-gate MOSFET model comprising quantum-mechanical and nonstatic effects. *IEEE Trans Electron Devices*, 1999, 46: 1656
- [16] Munteanu D, Autran J L, Loussier X, et al. Quantum short-channel compact modelling of drain current in double-gate MOSFET. *Solid-State Electron*, 2006, 50: 680
- [17] Ge L, Fossum J. Analytical modeling of quantization and volume inversion in thin Si-film double-gate MOSFETs. *IEEE Trans Electron Devices*, 2002, 49: 287
- [18] Winter R G. Quantum physics. Belmont, CA: Wadsworth, 1979
- [19] Lopez-Villanueva J A, Catujo-Cassinello P, Gámiz F, et al. Effects of the inversion-layer centroid on the performance of double-gate MOSFET's. *IEEE Trans Electron Devices*, 2000, 47: 141
- [20] Vasileska D, Ren Z. SCHRED-2.0 Manual. Tempe, AZ: Arizona State University Press, 2000